(1968).
[5]D. S. Falk, Phys. Rev. 118, 105 (1960).
[6]G. M. Gandel'mann and V. M. Ermachenko, Zh. Eksperim. i Teor. Fiz. 45, 522 (1963) [Soviet Phys. JETP, 18, 358 (1964)].
[7]D. R. Penn, Phys. Rev. 128, 2093 (1962).
[8]J. Lindhard and A. Winther, Kgl. Danske Videnskab. Selskab, Mat.-Fys. Medd. No. 34, 4 (1964).
[9]J. M. Ziman, *Principles of the Theory of Solids* (Cambridge, U. P., London, 1964), p. 138.
[10]C. B. Wilson, Proc. Phys. Soc. (London) 76, 481 (1960).
[11]E. S. Machlin, S. Petralia, A. Desalvo, R. Rosa, and F. Zignani, Phil. Mag. 22, 101 (1970).
[12]D. F. DuBois and M. G. Kivelson, Phys. Rev. 186, 409 (1969).
[13]G. Paasch, Phys. Status Solidi 38, K123 (1970).

PHYSICAL REVIEW B VOLUME 3, NUMBER 4 15 FEBRUARY 1971

# Calculation of the Temperature Dependence of the Energy Gaps in PbTe and SnTe†

Y. W. Tsang and Marvin L. Cohen
*Department of Physics, University of California, Berkeley, California* 94720
(Received 21 August 1970)

The empirical pseudopotential method is modified to calculate the temperature dependence of the first direct gap $E_g$ of PbTe at the $L$ point of the Brillouin zone. The same set of form factors which had given a reasonable band structure throughout the Brillouin zone and which adequately explains the optical properties of PbTe gives both the correct positive sign and magnitude for $(\partial E_g/\partial T)|_P$. The same method when applied to SnTe gives very unusual results, namely, a negative temperature coefficient for the region in the Brillouin zone near the minimum gap but a positive temperature coefficient for gaps slightly removed from the minimum gap. This appears to be consistent with the negative temperature coefficient obtained from tunneling experiments and the positive temperature coefficients obtained from optical measurements. The origin of the temperature dependence of conduction and valence levels at the gap is discussed in detail.

## I. INTRODUCTION

Optical experiments[1,2] at constant pressure show that the first direct gap $E_g$ of PbTe at the $L$ point of the Brillouin zone increases linearly with temperature in the temperature range 80–350 °K; for higher temperatures, the $E_g(T)$ curve approaches a constant value. The value of the linear temperature coefficient $(\partial E_g/\partial T)|_P$ in the linear region lies between[1,2] $4.1\times10^{-4}$ and $4.5\times10^{-4}$ eV(°K)$^{-1}$. The positive sign of the temperature coefficient is interesting since most semiconductors have a negative temperature coefficient. In this paper, a theoretical calculation[3] of $(\partial E_g/\partial T)|_P$ for PbTe using the pseudopotential method is outlined. We obtain the correct positive sign and a value of $3.9\times10^{-4}$ eV(°K)$^{-1}$ for $(\partial E_g/\partial T)|_P$ in the temperature range from 40 to 200 °K (Fig. 1); the slope of the theoretical curve $E_g(T)$ begins to decrease for temperature above 200 °K.

In SnTe, metal-insulator-semiconductor tunneling experiments[4] yield a negative temperature coefficient of $-2\times10^{-4}$ (°K)$^{-1}$ for the region near the minimum energy gap. This theoretical calculation of the temperature coefficient in SnTe gives a value of $-1.3\times10^{-4}$ eV (°K)$^{-1}$ for the gap at the $L$ point of the Brillouin zone. The band structure of SnTe resembles that of PbTe throughout the zone except at

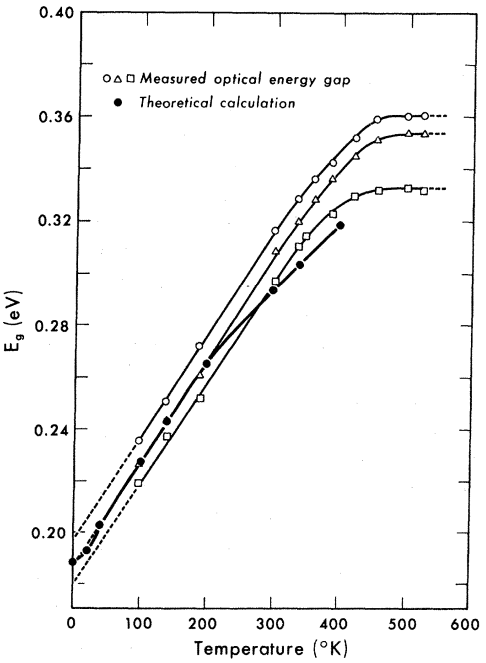


FIG. 1. Calculated and experimental temperature-dependent energy gap $E_g(T)$ for PbTe. The theoretical curve does not extend to high temperatures because Debye-Waller factors were not available above 400 °K. (The experimental data were taken from Ref. 1).

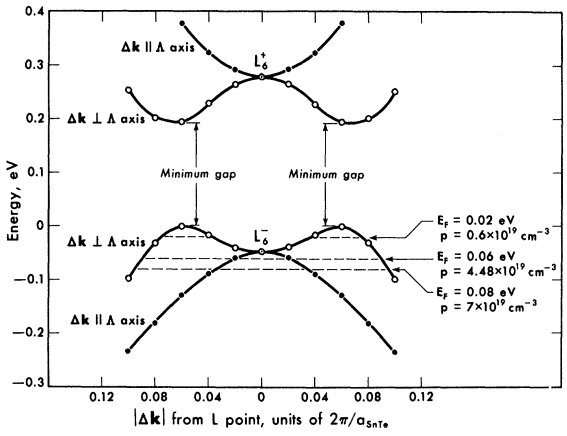


FIG. 2. Zero-temperature band structure for SnTe near $L$ for directions parallel and perpendicular to the $\Lambda$ axis showing both the first minimum gap near $L$ and the $L$ gap. Fermi levels corresponding to different hole concentrations $p$ are indicated.

and near the $L$ point. The symmetries of the top valence band and the bottom conduction band are $L_6^+$ and $L_6^-$, respectively, in PbTe; the ordering is reversed in SnTe, causing the calculated minimum gap to occur in the hexagonal face of the Brillouin zone,[5,6] slightly removed from $L$. For this reason, it is inadequate to discuss the temperature coefficient only at the $L$ point of the Brillouin zone for SnTe; rather, the temperature dependence of the gap in the region of the zone near $L$ should be taken into account. In Fig. 2 the valence- and conduction-band structure in the zone region near $L$ is displayed for $T=0°$, and the discussion of the temperature coefficient of SnTe will be given in Sec. IV.

## II. THEORY

The empirical pseudopotential method (EPM) band-structure calculation has been done[7,8] for PbTe and SnTe assuming zero temperature. The EPM calculation involved the determination of three symmetric pseudopotential form factors $V^S(G^2 = 4, 8, 12)$ and two antisymmetric form factors $V^A(G^2 = 3, 11)$; the reciprocal-lattice vector squared $G^2$ being expressed in units of $(2\pi/a)^2$, where $a$ is the lattice constant. At finite temperatures, band energies differ from their zero-temperature values because of two effects: (i) over-all expansion of the crystal, i.e., an increase in the lattice constant, and (ii) the thermal motion of the ion cores with a mean-squared ion displacement which we will call $\langle \delta R_\alpha^2 \rangle_{\rm av}$. The finite-temperature system, therefore, differs from the picture of a frozen lattice with all ion cores at their equilibrium positions ($\langle \delta R_\alpha^2 \rangle_{\rm av} = 0$) which was assumed in the zero-temperature calculation. In this calculation the EPM is modified to take both contributions into account at finite temperatures. The lattice constants $a(T)$ for various temperatures, in the range $T = 0$–$400\,°$K, are deduced from experiments[9,10] and tabulated in Table I. These are employed in the band-structure calculations at different temperatures. For the temperature dependence of energy bands arising from contribution (ii), we follow the theory of Yu[11] and Yu and Brooks[12] by including the Debye-Waller factor into the pseudopotential as follows.

The pseudopotential $V(\vec{G})$ in the reciprocal lattice is written as

$$V(\vec{G}) = \sum_\alpha S_\alpha(\vec{G})\, V_\alpha(\vec{G}) = \sum_\alpha e^{i\vec{G}\cdot\vec{\tau}_\alpha} V_\alpha(\vec{G}), \quad (1)$$

where $\vec{\tau}_\alpha$ is the position of the ion $\alpha$ with respect to an origin in the primitive cell. $V_\alpha(\vec{G})$ is the atomic pseudopotential and $S_\alpha(\vec{G})$ is the structure factor. [Often the quantity $\sum_\alpha S_\alpha(\vec{G})$ is also called the structure factor.] For the finite-temperature calculation, $S_\alpha(\vec{G})$ is replaced by a temperature-dependent structure factor

$$S_\alpha(\vec{G}, T) = e^{i\vec{G}\cdot\vec{\tau}_\alpha} e^{-W_\alpha(|\vec{G}|, T)} = e^{i\vec{G}\cdot\vec{\tau}_\alpha} e^{-G^2\langle \delta R_\alpha^2 \rangle_{\rm av}/2}, \quad (2)$$

where $e^{-W_\alpha(|\vec{G}|,T)}$ is the square root of the usual Debye-Waller factor related to the thermal average of the squared ion displacement $\langle \delta R_\alpha^2 \rangle_{\rm av}$.

## III. CALCULATION FOR PbTe

Keffer and co-workers[13-15] have calculated the temperature dependence of the energy gap using Debye-Waller factors of $e^{-W_{\rm Pb}}$ and $e^{-W_{\rm Te}}$ determined from (a) x-ray diffraction experiment at 300 °K and (b) values of $\langle \delta R_\alpha^2(T) \rangle_{\rm av}$ in the temperature range 0–400 °K calculated from phonon spectrum and polarization vectors obtained by Cochran *et al.*[16] In Table II we tabulate these results[13,15] at various temperatures for Pb and Te in PbTe. The tabulated results have a common zero-point contribution for

TABLE I. Lattice constants $a(T)$ for PbTe and SnTe determined from experiment (Refs. 9 and 10).

| Temperature (°K) | $a(T)$ (Å) SnTe | PbTe |
|---|---|---|
| 0 | 6.3130 | 6.454 |
| 20 | 6.3134 | 6.4543 |
| 40 | 6.3145 | 6.4556 |
| 80 | 6.3184 | 6.4595 |
| 100 | 6.3207 | 6.4624 |
| 140 | 6.3253 | 6.4675 |
| 200 | 6.3328 | 6.4751 |
| 240 | 6.3380 | 6.4802 |
| 300 | 6.3458 | 6.4879 |
| 340 | 6.3510 | 6.4929 |
| 400 | 6.3588 | 6.5006 |

TABLE II. Calculated average ion displacements $\langle \delta R_a^2 \rangle_{av}$ for PbTe and SnTe. (The values for PbTe were obtained from Refs. 13 and 15.)

| Temperature (°K) | $\langle \delta R_{Pb}^2 \rangle_{av}$ in PbTe (Å$^2$) | $\langle \delta R_{Te}^2 \rangle_{av}$ in PbTe (Å$^2$) | $\langle \delta R_{Sn}^2 \rangle_{av}$ in SnTe (Å$^2$) | $\langle \delta R_{Te}^2 \rangle_{av}$ in SnTe (Å$^2$) |
|---|---|---|---|---|
| 0 | 0 | 0 | 0 | 0 |
| 20 | 0.0006 | 0.0002 | | |
| 40 | 0.002 | 0.008 | 0.008 | 0.007 |
| 80 | | | 0.0026 | 0.0021 |
| 100 | 0.007 | 0.0036 | 0.0036 | 0.0030 |
| 140 | 0.0105 | 0.0056 | | |
| 200 | 0.0157 | 0.0086 | 0.0089 | 0.0072 |
| 240 | 0.0192 | 0.0107 | | |
| 300 | 0.0244 (x-ray measurement gives 0.0331) | 0.0138 (x-ray measurement gives 0.0177) | 0.0142 | 0.0116 |
| 340 | 0.0279 | 0.0159 | | |
| 400 | 0.0332 | 0.0189 | 0.0196 | 0.0160 |

each $\langle \delta R_a^2(T) \rangle_{av}$ subtracted out. This subtraction occurs because the EPM determination of the band energies at $T = 0$ °K involves potentials obtained by fitting a few gaps to optical reflectivity experiments and therefore already contains the zero-point motion. With the lattice constants $a(T)$ and the calculated Debye-Waller factor $e^{-W_\alpha(|\vec{G}|,T)}$, the finite-temperature band energies of PbTe at the $L$ point of the Brillouin zone are calculated. The set of form factors used for each temperature of interest is merely scaled by an interpolation scheme from the set used for the zero-temperature calculation with no additional parameters or adjustments. The pseudopotential form factors

$$V^S(\vec{G}) = (1/\Omega)[\int V_{Pb}(|\vec{r}|)\, e^{-i\vec{G}\cdot\vec{r}} d^3r + \int V_{Te}(|\vec{r}|)\, e^{-i\vec{G}\cdot\vec{r}} d^3r], \quad (3a)$$

$$V^A(\vec{G}) = (1/\Omega)[\int V_{Pb}(|\vec{r}|)\, e^{-i\vec{G}\cdot\vec{r}} d^3r - \int V_{Te}(|\vec{r}|)\, e^{i\vec{G}\cdot\vec{r}} d^3r] \quad (3b)$$

scale according to $|\vec{G}|$ (units of $2\pi/a$) in the exponential as well as in the volume factor $\Omega = \frac{1}{4}a^3$. The atomic pseudopotential in real space $V_\alpha(|\vec{r}|)$ is assumed to be independent of temperature in the scaling process, which is the rigid-ion assumption. Specifically, the interpolation and scaling procedure involves (a) taking the zero-temperature symmetric form factors[7,8] (in Ry) $V^S(G^2=4) = -0.241$, $V^S(8) = -0.0352$, $V^S(12) = 0.017$, $V^S(16) = 0$; (b) fitting a smooth curve $V(q)$ with a polynomial of order three to these points; (c) reading off the values of $V^S$ at $G^2(T) = 4, 8, 12$ [$G^2$ is implicitly a function of temperature through the lattice constant $a(T)$]; and (d) scaling each value of $V^S$ by $a^3(0)/a^3(T)$. The same procedure applies to the antisymmetric form factors (in Ry) $V^A(G^2=3) = 0.052$, $V^A(11) = 0.021$, $V^A(16) = 0$. In addition, since $W_{Pb}(|\vec{G}|, T)$ is not equal to $W_{Te}(|\vec{G}|, T)$, the property of the vanishing of symmetric structure factor for odd $|\vec{G}|^2$ and antisymmetric form factors for even $|\vec{G}|^2$ (as discussed for the zero-temperature case[8,17] is no longer valid. For finite temperatures, $V^S(|\vec{G}|^2 = 3, 11)$ and $V^A(|\vec{G}|^2 = 4, 8, 12)$ are needed, in addition to the five required for the zero-temperature calculation, namely, $V^S(|\vec{G}|^2 = 4, 8, 12)$ and $V^A(|\vec{G}|^2 = 3, 11)$. These five additional form factors are again obtained by the interpolation and extrapolation scheme from the original five with no arbitrary adjustment.

Figure 1 shows both the calculated PbTe $E_g(T)$ vs temperature and that obtained from experiment.[1] The nonlinear temperature dependence of the gap below 40 °K is a result of the temperature dependence of the expansion coefficient

$$\alpha = \frac{1}{3V}\left.\frac{\partial V}{\partial T}\right|_P$$

at low temperatures ($V$ being the volume). In the temperature range 40–200 °K, the theoretical temperature dependence

$$\left.\frac{\partial E_g}{\partial T}\right|_P = 3.9\times10^{-4}\ \text{eV}(^\circ\text{K})^{-1}$$

is in agreement with the experimental value of $4.1 \times 10^{-4}\,\text{eV}(^\circ\text{K})^{-1}$. Above 200 °K the slope of the theoretical $E_g(T)$ curve decreases, but the experimental slope of $4.1\times10^{-4}\,\text{eV}(^\circ\text{K})^{-1}$ persisted up to about 350 °K; the theoretical temperature coefficient between the two temperatures 100 °K and 300 °K is only $3.3\times10^{-4}\,\text{eV}(^\circ\text{K})^{-1}$.

In order to gain a better understanding of the deviation of theoretical result from experiment for the temperature coefficient, the calculation was redone to examine the two principal contributions:

the lattice effect and the Debye-Waller effect. These two contributions were separated and examined in turn. Since the two convenient variables for the theoretical calculation of band energies are volume $V$ and temperature $T$, the temperature coefficient for the energy gap $E_g(V, T)$ at constant pressure is

$$\left.\frac{\partial E_g(V,T)}{\partial T}\right|_P = \left.\frac{\partial E_g(V,T)}{\partial V}\right|_T \left.\frac{\partial V}{\partial T}\right|_P + \left.\frac{\partial E_g(V,T)}{\partial T}\right|_V ; \tag{4}$$

the first term in Eq. (4) accounts for the lattice effect, the second term accounts for the thermal motion or Debye-Waller effect. To obtain only the first term in Eq. (4), one scales the five zero-temperature form factors to values corresponding to lattice constants at $T = 100\,^\circ\mathrm{K}$ and $T = 300\,^\circ\mathrm{K}$, obtaining

$$[E_g(T = 300\,^\circ\mathrm{K}) - E_g(T = 100\,^\circ\mathrm{K})]/200\,^\circ\mathrm{K} = 1.8\times10^{-4}\ \mathrm{eV}(^\circ\mathrm{K})^{-1} . \tag{5}$$

The value of $1.7\times10^{-4}\ \mathrm{eV}(^\circ\mathrm{K})^{-1}$ is obtained if the experimentally measured pressure dependence of the energy gap, compressibility, and expansion coefficient $[\alpha = (1/3V)(\partial V/\partial T)|_P$ is constant above $T = 100\,^\circ\mathrm{K}$ and has the value $1.97\times10^{-6}(^\circ\mathrm{K})^{-1}]$ are used The agreement between the theoretical and experimental results is therefore very good for the lattice effect. To examine the second term in Eq. (4), the calculated Debye-Waller factors for $T = 100\,^\circ\mathrm{K}$ and $300\,^\circ\mathrm{K}$ were put into the structure factors. Zero-temperature form factors and lattice constant were used. The resultant gap temperature dependence arising from the Debye-Waller effect alone is

$$\left.\frac{\partial E_g(V,T)}{\partial T}\right|_V = 1.3\times10^{-4}\ \mathrm{eV}(^\circ\mathrm{K})^{-1} . \tag{6}$$

A value of $2.4\times10^{-4}\ \mathrm{eV}(^\circ\mathrm{K})$ would be expected from experiment. The above analysis indicated that the discrepancy between theory and experiment arises mainly from the Debye-Waller effect. In Table II it is seen that $\langle \delta R_a^2 \rangle_{av}$ (at $300\,^\circ\mathrm{K}$) from measured x-ray experiments is different from that which was calculated from phonon data (used in this temperature-dependent calculation). With the Debye-Waller factor derived from this x-ray determination of $\langle \delta R_a^2 \rangle_{av}$ at $300\,^\circ\mathrm{K}$, one obtains a gap almost 0.02 eV larger than that obtained before; this factor alone could change the resultant $(\partial E_g/\partial T)|_P$ by as much as $1\times10^{-4}\ \mathrm{eV}(^\circ\mathrm{K})^{-1}$, which is enough to bring the theoretical result into excellent agreement with the experimentally determined value.

## IV. CALCULATION FOR SnTe

The procedure employed for PbTe is followed closely in the calculation for SnTe. The lattice constant in the temperature range 0–400 °K is obtained from the experimental thermal expansion coefficient $\alpha(T)$, [10] and the form factors are scaled according to the respective lattice constants at various temperatures. The zero-temperature form factors are those given in Refs. 7 and 8. However, a complete listing of polarization vectors from the phonon spectrum is not available for the computation of $\langle \delta R_{\mathrm{Sn}}^2 \rangle_{av}$ and $\langle \delta R_{\mathrm{Te}}^2 \rangle_{av}$ as in the PbTe calculation. Instead, the mean-squared displacements were calculated from the frequency distributions of Sn and Te motion[18] (the frequency distributions are the sums of polarization vectors over phonon modes $t$ and wave vector $\vec{q}$)

$$\sum_{t,\vec{q}} |\vec{e}_{\vec{q},t}(\mathrm{Sn})|^2, \qquad \sum_{t,\vec{q}} |\vec{e}_{\vec{q},t}(\mathrm{Te})|^2 ,$$

respectively, in each frequency range; the polarization $\vec{e}_{\vec{q},t}(\mathrm{Sn})$ is defined by

$$\delta\vec{R}_{\mathrm{Sn}} = \sum_{\vec{q},t} \left(\frac{\hbar}{2MN\omega_{\vec{q}}}\right)^{1/2} \vec{e}_{\vec{q},t}(\mathrm{Sn})(a_{\vec{q}}\, e^{i\vec{q}\cdot\vec{R}_{\mathrm{Sn}}} + a_{\vec{q}}^{+}\, e^{-i\vec{q}\cdot\vec{R}_{\mathrm{Sn}}}) . \tag{7}$$

The calculated mean-squared displacements for Sn and Te as a function of temperature are tabulated in Table II, together with those of PbTe.

The total temperature coefficient of the $L$ gap is $-1.3\times10^{-4}\ \mathrm{eV}(^\circ\mathrm{K})^{-1}$ between temperatures 100 and 300 °K. A graph of $E_g(T)$ vs temperature in the temperature range 0–400 °K is given in Fig. 3. The band structure near the $L$ gap had been shown to be complicated.[5,6,8] Figure 2 gives the zero-temperature band structure near $L$[5] in directions both parallel and perpendicular to the $\Lambda$ axis near $L$. It is clear that the first minimum gap in SnTe is in the hexagonal face of the Brillouin zone perpendicular

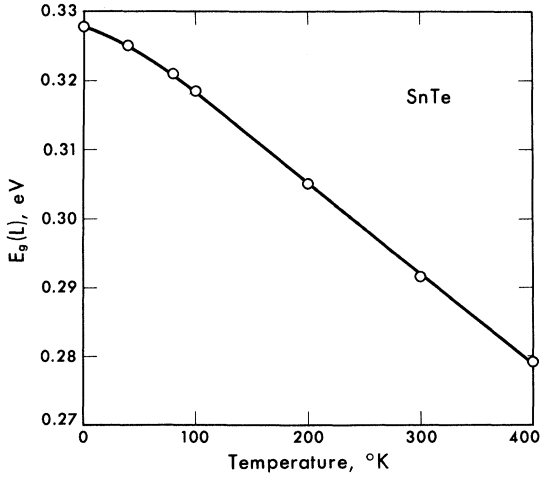


FIG. 3. Calculated temperature-dependent energy gap $E_g(T)$ at $L$ for SnTe.

to the $\Lambda$ axis; the second smallest gap is at $L$. In Table III the values of energy gaps (for $T=0$ and 400 °K) for $\vec{k}$ near $L$ along and perpendicular to $\Lambda$ are tabulated. The gap decreases with increasing temperatures for all $k$ values lying between the gap at $L$ and the first minimum gap. The magnitudes of the temperature coefficients, however, are small and decrease with increasing distance from the $L$ point.

The temperature coefficient becomes positive with $k$ values beyond the first minimum; or, using the language of a previous paper, [5] beyond the hump structure. This result is anticipated from the band structure of SnTe calculated previously by the EPM[5,7] and by the augmented-plane-wave method.[19] Dimmock *et al.*[20] originally proposed the reversal of band ordering at $L$ from PbTe to SnTe. If one explores (using a simple perturbation model) what happens as one goes from the PbTe band ordering at $L$ to that of SnTe, the bands would cross at the hump structure (Fig. 2) if they did not interact with each other. The bands, however, do repel each other, thus forming gaps at this point. Because of the larger band mass along the $\Lambda$ direction, the hump structure does not appear along this direction. With this model, the SnTe valence band at $L$ within the humps in the direction perpendicular to $\Lambda$ comes from the piece of conduction band connected with $L_6^-$ in the PbTe structure; whereas, the SnTe conduction band within the humps arises from the PbTe valence-band structure connected with $L_6^+$. Outside the humps, the PbTe and SnTe band-structure symmetry is the same. The temperature dependence of the gap near $L$ in PbTe is positive because one level is more sensitive than the other to temperature. Specifically,

$$\left.\frac{\partial E}{\partial T}\right|_{\vec{p}}^{\text{upper level}} - \left.\frac{\partial E}{\partial T}\right|_{\vec{p}}^{\text{lower level}} > 0 \,. \tag{8}$$

With the further assumption that each band edge connected with $L_6^+$, $L_6^-$, respectively, in the PbTe-like structure, moves as a whole with temperature, it is clear that in the SnTe structure, the gap temperature coefficient will have the same sign as PbTe outside the humps, but an opposite sign within the humps. Esaki and Stiles[4] had reported that the minimum gap in SnTe has a temperature coefficient of about $-2\times10^{-4}$ eV(°K)$^{-1}$ between 4.2 and 100 °K. Burke and Riedl[21] have obtained apparently contradictory results for the temperature coefficient of the direct gaps for the photon-energy regions 0.35 eV–0.65 eV, using optical data. They obtained a small negative temperature coefficient [0 to $-1.5\times10^{-4}$ eV (°K)$^{-1}$] for photon energies below 0.4 eV; above this photon energy, a positive temperature coefficient is obtained. Because of the thermal broadening of the Fermi level, the experimental photon energies given may not[21] correspond directly to the direct gap in the band-structure calculation. However, there is no question that these data strongly suggest gaps having positive temperature coefficient near the band edge. Only states very close to the band edge will have a negative temperature coefficient, in agreement with the tunneling experiments[4] and the results of this calculation.

The value of the Fermi level as a function of carrier concentration in SnTe (according to the EPM) has been previously computed.[8] In Fig. 2 this information is entered on the zero-temperature valence-band structure. Note the small calculated $E_F$. It is clear from the figure that a carrier concentration of about $7\times10^{19}$ cm$^{-3}$ will give a gap that has a positive temperature coefficient. For the carrier concentration of $3.6\times10^{19}$ cm$^{-3}$ used in optical gap experiments,[21] the Fermi level falls between the levels given in Fig. 2, somewhat below the $L$ point. Table III shows that the temperature coefficient at this point ($\Delta\vec{k}$ is about $0.08\,2\pi/a$ from $L$) is almost zero. This theoretical calculation of the temperature dependence near the band edge in SnTe therefore gives a consistent picture of the present experimental situation.

Table III shows that a negative gap temperature coefficient is obtained from the $\Lambda$ direction near $L$. This results from the large mass along $\Lambda$. The de-

TABLE III. Energy-gap values for SnTe near $L$ for $T=0$ °K and $T=400$ °K. $\Delta\vec{k}$'s are measured from the $L$ point of the Brillouin zone.

| $\lvert\Delta\vec{k}\rvert$ (units of $2\pi/a$) | $E_g$ for direction $\perp\Lambda$ axis | | $E_g$ for direction $\parallel\Lambda$ axis | |
|---|---|---|---|---|
| | $E_g^{\perp}(T=0\,°\mathrm{K})$ | $E_g^{\perp}(T=400\,°\mathrm{K})$ | $E_g^{\parallel}(T=0\,°\mathrm{K})$ | $E_g^{\parallel}(T=400\,°\mathrm{K})$ |
| (Å$^{-1}$) | (eV) | (eV) | (eV) | (eV) |
| 0 | 0.327 | 0.279 | 0.327 | 0.279 |
| 0.02 | 0.304 | 0.258 | 0.35 | 0.305 |
| 0.04 | 0.244 | 0.201 | 0.412 | 0.374 |
| 0.06 | 0.195 | 0.168 | 0.51 | 0.464 |
| 0.08 | 0.232 | 0.229 | 0.628 | 0.566 |
| 0.10 | 0.349 | 0.359 | 0.756 | 0.675 |
| 0.12 | 0.497 | 0.506 | | |

termination of energy gaps by optical experiments involves direct transitions from all the holes on the Fermi surface, which according to this analysis includes regions of both positive and negative temperature coefficients. The measured temperature coefficient will be an average over the Fermi surface. A previous calculation[8,22] which maps out the Fermi surface demonstrates the complexity of the surface and it is not obvious which sign of the gap temperature coefficient will dominate at a given carrier concentration. Therefore, the comparison of this calculation with the optical experiments is only qualitative. The tunneling experiments, however, explore the region near the minimum gap. The magnitude of the calculated temperature coefficient at the minimum gap is small compared with the experimental values. The discrepancy, we believe, again arises from the uncertainty in the set of Debye-Waller factors used in the calculation, as will be discussed in Sec. V.

## V. DISCUSSION FOR PbTe AND SnTe

It is easier to analyze the above calculation for SnTe if the two principal contributions to the temperature coefficient (lattice effect and Debye-Waller effect) are examined separately, as was done in Sec. III for PbTe.

Lattice effect will be dealt with first. Table IV gives the shift of the energy levels at the $L$ point of the Brillouin zone from $T=100\,^\circ$K to $T=300\,^\circ$K. [100 and 300 °K are chosen because they are within the temperature range where the expansion coefficient $\alpha=(1/V)(\partial V/\partial T)|_P$ can be taken to be linear.] With increasing temperature, the lattice constant expands, thus reducing the kinetic-energy term $\hbar^2|\vec{k}+\vec{G}|^2/2m$ in the pseudopotential Hamiltonian matrix element. This accounts for the negative temperature coefficient of each individual level in both SnTe and PbTe. The magnitude of the temperature coefficient for each individual level is of the same order in both SnTe and PbTe, with the exception of the $L_6^+$ level at the gap. This $L_6^+$ level is more sensitive to the lattice change than the other levels. It forms the top valence band in PbTe and the bottom conduction band in SnTe, thus giving a positive gap temperature coefficient in PbTe and a coefficient of opposite sign in SnTe. The gap coefficient arising only from the lattice effect is $1.8\times10^{-4}$ eV(°K)$^{-1}$ in PbTe and $-2.8\times10^{-4}$ eV(°K)$^{-1}$ in SnTe. The ordering of the gap is crucial in giving the correct signs of this lattice part of the temperature coefficient in SnTe and PbTe. For this contribution pseudopotentials in SnTe and PbTe only slightly affect the temperature coefficient of the levels.

TABLE IV. Temperature coefficients between $T=100\,^\circ$K and 300 °K arising only from the lattice effect for the $L$ levels in SnTe and PbTe. The labels *cb* and *vb* refer to conduction bands and valence bands.

| SnTe | | PbTe | |
|---|---|---|---|
| Symmetry | $E(T=300\,^\circ\text{K})-E(T=100\,^\circ\text{K})$ (eV) | Symmetry | $E(T=300\,^\circ\text{K})-E(T=100\,^\circ\text{K})$ (eV) |
| $L_6^-(cb)$ | -0.09 | $L_6^-(cb)$ | -0.083 |
| $L_6^+(cb)$ | -0.142 | $L_6^-(cb)$ | -0.088 |
| gap | | gap | |
| $L_6^-(vb)$ | -0.088 | $L_6^+(vb)$ | -0.124 |
| $L_{45}^+(vb)$ | -0.083 | $L_{45}^+(vb)$ | -0.076 |
| $L_6^+(vb)$ | -0.096 | $L_6^+(vb)$ | -0.091 |

TABLE V. SnTe temperature coefficients between $T=100$ and 300 °K arising only from the Debye-Waller effect for the $L_6^+$ and $L_6^-$ levels and $E_g$.

| $\langle\delta R_{\text{Te}}^2\rangle_{\text{av}}$ (Å) | $\left.\frac{\partial L_6^+}{\partial T}\right\|_V$ ($10^{-4}$ eV/°K) | $\langle\delta R_{\text{Sn}}^2\rangle_{\text{av}}$ (Å) | $\left.\frac{\partial L_6^-}{\partial T}\right\|_V$ ($10^{-4}$ eV/°K) | $\left.\frac{\partial E_g}{\partial T}\right\|_V=\left.\frac{\partial(L_6^+-L_6^-)}{\partial T}\right\|_V$ ($10^{-4}$ eV/°K) |
|---|---|---|---|---|
| 0.0116 | 4.88 | 0.0142 | 3.51 | + 1.37 |
| 0.0116 | 4.74 | 0.0232 | 5.45 | - 0.71 |
| 0.0116 | 4.94 | 0.0058 | 1.54 | + 3.4 |
| 0.0024 | 1.02 | 0.0036 | 0.78 | + 0.24 |
| 0.0024 | 0.99 | 0.0048 | 1.26 | - 0.27 |
| 0.0024 | 1.07 | 0.0012 | 0.33 | + 0.74 |

The Debye-Waller effect will be discussed next. The $L_6^+$ and $L_6^-$ levels at the gap come from the single-group symmetry $L_1$ and $L_2$, respectively. These symmetries imply that the $L_6^+$ level is $s$-like about Sn or Pb and $p$-like about Te, whereas, $L_6^-$ is $s$-like about Te and $p$-like about Sn or Pb. The Debye-Waller factor $e^{-G^2\langle\delta R_\alpha^2\rangle_{\text{av}}/2}$ deals with the mean-squared displacement of the ion cores from the rigid-lattice positions. Intuitively, one would correlate the $p$ character of an energy level and a sensitivity to temperature arising from the Debye-Waller effect since the movement of the atom brings it into contact with the electron density away from the core. The $s$ character in the energy level is expected not to be sensitive to changes in $\langle\delta R_\alpha^2\rangle_{\text{av}}$ because of the spherical symmetry. Table V verifies this prediction. The first row of this table tabulates the three temperature coefficients between $T=100$ and 300 °K for SnTe

$$\left.\frac{\partial L_6^+}{\partial T}\right|_V,\quad \left.\frac{\partial L_6^-}{\partial T}\right|_V,\quad \text{and}\quad \left.\frac{\partial E_g}{\partial T}\right|_V$$

where

$$E_g=L_6^+-L_6^-$$

for SnTe, and the mean-squared displacements $\langle\delta R_{\text{Sn}}^2\rangle_{\text{av}}$ and $\langle\delta R_{\text{Te}}^2\rangle_{\text{av}}$ for $T=300\,^\circ$K. In the second and third row $\langle\delta R_{\text{Sn}}\rangle_{\text{av}}$ is artifically varied to double and half of the mean-squared displacement of

Te, keeping $\langle \delta R^2_{Te} \rangle_{av}$ constant. The resultant temperature coefficients with this change in $\langle \delta R^2_{Sn} \rangle_{av}$ are then tabulated. These values indicate that the temperature coefficient of the energy level $L_6^-$ which is $p$-like about Sn changes with the artifical changes imposed on $\langle \delta R^2_{Sn} \rangle_{av}$. The temperature coefficient of the $L_6^+$ energy level which is $p$-like about Te remains essentially unchanged. The above procedure is now repeated for small values of $\langle \delta R^2_{Te} \rangle_{av}$ and $\langle \delta R^2_{Sn} \rangle_{av}$ in rows four, five, and six. An arbitrary value of approximately one-fifth of the value calculated from Cowley's[18] phonon spectrum is chosen for $\langle \delta R^2_{\alpha} \rangle_{av}$ in row four. In the fifth and sixth rows of Table V we list the temperature coefficients resulting from a variation of $\langle \delta R^2_{Sn} \rangle_{av}$ to double and half that of $\langle \delta R^2_{Te} \rangle_{av}$ in row four. The temperature coefficients $(\partial L_6^+/\partial T)|_V$ and $(\partial L_6^-/\partial T)|_V$ of row four clearly are a factor of 4 to 5 smaller than that of row one. The temperature coefficient $(\partial L_6^+/\partial T)|_P$ of rows four, five, and six again remains quite constant.

This point is made most clearly using a graph. In Fig. 4 the solid curve represents $(\partial L_6^-/\partial T)|_V$ vs $\langle \delta R^2_{Sn} \rangle_{av}$ ($T = 300\,^\circ$K) and the dash curve plots $(\partial L_6^+/\partial V)|_V$ vs $\langle \delta R^2_{Te} \rangle_{av}$ ($T = 300\,^\circ$K). This figure clearly indicates the following:

(a) $(\partial L_6^-/\partial T)|_V$ is linearly proportional to $\langle \delta R^2_{sn}(T) \rangle_{av}$, that is,

$$(\partial L_6^-/\partial T)\big|_V = \beta_-(T)\langle \delta R^2_{Sn}(T)\rangle_{av} + \delta_- ; \tag{9}$$

(b) $(\partial L_6^+/\partial T)|_V$ is linearly proportional to $\langle \delta R^2_{Te}(T) \rangle_{av}$, that is,

$$(\partial L_6^+/\partial T\big|_V = \beta_+(T)\langle \delta R^2_{Te}(T)\rangle_{av} + \delta_+ ; \tag{10}$$

(c) the slopes $\beta_+(T)$ and $\beta_-(T)$ are both positive and $\beta_+(T) > \beta_-(T)$.

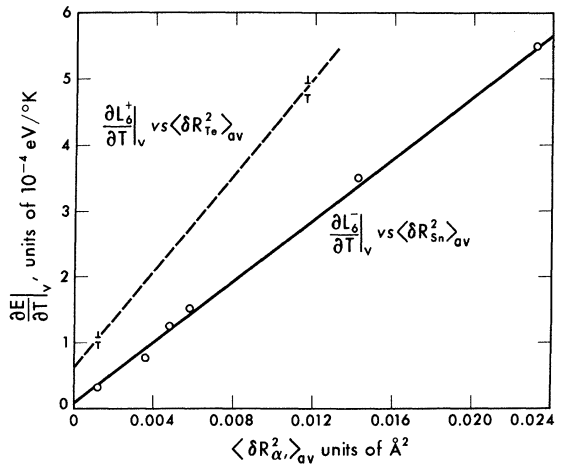


FIG. 4. Graph of temperature coefficients $(\partial L_6^+/\partial T)|_V$ and $(\partial L_6^-/\partial T)|_V$ vs $\langle \delta R^2_{Te} \rangle_{av}$ ($T = 300\,^\circ$K) and $\langle \delta R^2_{Sn} \rangle_{av}$ ($T = 300\,^\circ$K), respectively. (The brackets on the dash curve show the range of values of $(\partial L_6^+/\partial T)|_V$ given in Table V.)

Properties (a) and (b) can be partially arrived at by symmetry considerations alone. The temperature coefficients of individual level $(\partial L_6^+/\partial T)|_V$, $(\partial L_6^-/\partial T)|_V$, etc., are all positive because the increased vibrations of the ion cores adds extra energy to the system. In case (c) the observation that $\beta_+(T)$ is greater than $\beta_-(T)$ may be attributed to the fact that Te probably has more affinity for the valence electrons. The same property holds for PbTe; the exact values of $\beta_+(T)$ and $\beta_-(T)$, however, are very much dependent on the pseudopotential form factors used.

With the former analysis, the temperature dependence of PbTe and SnTe is completely consistent. For PbTe at the $L$ point, $L_6^-$ forms the conduction band and $L_6^+$ the valence band. For the lattice effect, all levels move down with increasing temperature, but $L_6^+$ is more sensitive, thus giving rise to a positive gap temperature coefficient. For the Debye-Waller effect, all levels move up with increasing temperature. If $\langle \delta R^2_{Pb} \rangle_{av}$ and $\langle \delta R^2_{Te} \rangle_{av}$ were the same, property (c) would predict that the $L_6^+$ moves up more than the $L_6^-$ in a given temperature range. However, Table II shows that $\langle \delta R^2_{Pb} \rangle \gg \langle \delta R^2_{Te} \rangle_{av}$ for each temperature, thus compensating for the smaller slope $\beta_-(T)$ for the $L_6^-$ level. The result is that the $L_6^-$ actually moves up more than $L_6^+$, giving a positive gap temperature coefficient.

SnTe has the opposite band ordering at the $L$ point, $L_6^+$ on top and $L_6^-$ on the bottom. For the lattice part, $L_6^+$ is again sensitive and moves down more than the $L_6^-$ for a given temperature range, thus giving rise to a negative gap temperature coefficient of $-2.8\times10^{-4}$ eV(°K)$^{-1}$. For the Debye-Waller effect, all levels move up. Since $\langle \delta R^2_{Sn} \rangle_{av}$ is only slightly greater than $\langle \delta R^2_{Te} \rangle_{av}$ (Table II), it is not big enough to compensate for the larger slope $\beta_+(T)$. Therefore, the $L_6^+$ level moves up more than the $L_6^-$ level and gives a positive temperature coefficient for the Debye-Waller effect. The total temperature coefficient of the gap includes both the lattice and the Debye-Waller effect. The theoretical calculation gives $-1.3\times10^{-4}$ eV(°K)$^{-1}$ at $L$ for SnTe and much smaller magnitude for states near the minimum gap. Tunneling experiments yield a temperature coefficient which is approximately $-2\times10^{-4}$ eV(°K)$^{-1}$. The actual Debye-Waller factor used in this calculation has a large influence on the temperature coefficient. In the calculation for PbTe, it was found that whereas the Debye-Waller factors deduced from x-ray experiments and phonon calculations (involving phonon polarization vectors throughout the Brillouin zone) both give $\langle \delta R^2_{Pb} \rangle_{av} \gg \langle \delta R^2_{Te} \rangle_{av}$ a spherical-model calculation based on PbTe phonon frequency spectrum along symmetry directions gives $\langle \delta R^2_{Te} \rangle_{av}$

$\gg \langle \delta R_{Pb}^2 \rangle_{av}$. This set of Debye-Waller factors from the spherical model will give rise to a negative temperature coefficient in PbTe, contrary to experiment. For SnTe, a complete set of phonon polarization vectors and frequency throughout the Brillouin zone is not available. Therefore, the set of Debye-Waller factors used in the above calculation is deduced from the phonon frequency distribution (see Sec. IV). The results were similar to the Debye-Waller factors obtained from the spherical model. Should phonon polarization vectors be available for SnTe it would be interesting to investigate the Debye-Waller factors deduced from these measurements to recalculate the temperature dependence of SnTe.

## VI. SUMMARY

In summary, this calculation has shown that: (i) The set of zero-temperature pseudopotential form factors which gives a reasonable band structure throughout the Brillouin zone, and which adequately explains the optical properties of PbTe [7,8,22] also yields, in this finite-temperature calculation, both the correct sign and magnitude of the temperature coefficient of the direct gap at $L$. A similar calculation for SnTe near the $L$ region gives the correct sign but less satisfactory results for the magnitude of the temperature coefficients. (ii) The different gap ordering at $L$ is crucial to give opposite signs for the lattice contribution to the temperature coefficients in SnTe and PbTe. (iii) Reliable Debye-Waller factors are necessary in this type of calculation to give a quantitative description of the temperature-dependent band structure. (iv) Similar calculations have been done for GaAs [23] in excellent agreement with experiment. The success for GaAs and the fact that the set of form factors for PbTe gives good agreement with experiment for the lattice-expansion contribution to the temperature coefficient indicate that the discrepancy between theory and experiment for the total temperature coefficient might be accounted for by the uncertainty in the Debye-Waller factors. This adds further evidence for the usefulness of the EPM for gaining information about the temperature variation of band energies. Furthermore, since the temperature coefficient is sensitive to the choice of form factors, this kind of calculation serves to indicate how good the form factors are, and puts an additional constraint on the pseudopotential form factors.

## ACKNOWLEDGMENTS

We thank Professor A. Bienenstock and Dr. C. Keffer for kindly supplying us with the Debye-Waller factors, and for helpful comments. The phonon frequency spectrum for SnTe supplied by Dr. E. R. Cowley is gratefully acknowledged.

---

†Supported by the National Science Foundation.

[1]R. N. Tauber, A. A. Machonis, and I. B. Cadoff, J. Appl. Phys. 37, 4855 (1966).

[2]V. Prakish, Ph. D. thesis, Harvard University, Cambridge, Mass., 1967 (unpublished).

[3]Part of this calculation is similar to the calculation of Keffer, Hayes, and Bienenstock (see Refs. 13–15). These authors use pseudopotentials which are varied to give the appropriate levels only at the $L$ point of the Brillouin zone. The present calculation uses pseudopotentials which are constrained to give bands throughout the zone which yield optical constants consistent with experiment.

[4]L. Esaki and P. J. Stiles, Phys. Rev. Letters 16, 1108 (1966); P. J. Stiles, J. Phys. (Paris) 29, 105 (1968).

[5]Y. W. Tung and M. L. Cohen, Phys. Letters A29, 236 (1969).

[6]Preliminary experimental confirmation of our model is given in R. S. Allgaier, Bull. Am. Phys. Soc. 15, 304 (1970).

[7]Y. W. Tung and M. L. Cohen, Phys. Rev. 180, 823 (1969); M. L. Cohen, Y. Tung, and P. B. Allen, J. Phys. (Paris) 29, 163 (1968).

[8]Y. W. Tsang, Ph. D. thesis, University of California, Berkeley, Calif., 1970 (unpublished).

[9]B. Houston, R. E. Strakna, and A. S. Belson, J. Appl. Phys. 39, 3913 (1968).

[10]S. I. Novikova and L. E. Shelimova, Fiz. Tverd. Tela 7, 2544 (1965) [Soviet Phys. Solid State 7, 2052 (1966)].

[11]S. C. Yu, Ph. D. thesis, Harvard University, Cambridge, Mass., 1964 (unpublished).

[12]S. C. Yu and H. Brooks (unpublished).

[13]C. Keffer, Ph. D. thesis, Harvard University, Cambridge, Mass., 1969 (unpublished).

[14]C. Keffer, T. M. Hayes, and A. Bienenstock, Phys. Rev. Letters 21, 1677 (1968).

[15]C. Keffer, T. M. Hayes, and A. Bienenstock, Phys. Rev. B 2, 1966 (1970).

[16]W. Cochran, R. A. Cowley, G. Dolling, and M. M. Elcombe, Proc. Roy. Soc. (London) A293, 433 (1966).

[17]M. L. Cohen and T. K. Bergstresser, Phys. Rev. 141, 789 (1966). M. L. Cohen and V. Heine, *Solid State Physics*, edited by H. Ehrenreich, F. Seitz, and D. Turnbull (Academic, New York, 1970), Vol. 24.

[18]E. R. Cowley, J. K. Darby, and G. S. Pawley, J. Phys. C. 2, 1916 (1969). E. R. Cowley kindly supplied us with the separate frequency distributions for Sn and Te motions.

[19]S. Rabii, Phys. Rev. 182, 821 (1969).

[20]J. O. Dimmock, I. Melngailes, and A. J. Strauss, Phys. Rev. Letters 16, 1193 (1966).

[21]J. R. Burke, Jr., and H. R. Riedl, Phys. Rev. 184, 830 (1969).

[22]M. L. Cohen and Y. W. Tsang, J. Phys. Chem. Solids (to be published).

[23]J. P. Walter, R. R. L. Zucca, M. L. Cohen, and Y. R. Shen, Phys. Rev. Letters 24, 102 (1970).